



# Activated carbons of pistachio and acorn shells for supercapacitor electrodes with TEABF<sub>4</sub>/PC solutions as electrolytes

M. S. S. Faisal<sup>1</sup> · F. Abedin<sup>2</sup> · R. Asmatulu<sup>1</sup>

Received: 23 July 2019 / Revised: 9 October 2019 / Accepted: 1 January 2020 / Published online: 14 January 2020  
© Korean Carbon Society 2020

## Abstract

The energy demands of the world have been accelerating drastically because of the technological development, population growth and changing in living conditions for a couple of decades. A number of different techniques, such as batteries and capacitors, were developed in the past to meet the demands, but the gap, especially in energy storage, has been increasing substantially. Among the other energy storage devices, supercapacitors have been advancing rapidly to fill the gap between conventional capacitors and rechargeable batteries. In this study, natural resources such as pistachio and acorn shells were used to produce the activated carbons for electrode applications in a supercapacitor (or an electrical double-layer capacitor—EDLC). The activated carbon was synthesized at two different temperatures of 700 °C and 900 °C to study its effect on porosity and performance in the supercapacitor. The morphology of the activated carbon was studied using scanning electron microscopy (SEM). A solution of tetraethylammonium tetrafluoroborate (TEABF<sub>4</sub>)/propylene carbonate (PC) was prepared to utilize in supercapacitor manufacturing. The performance of the EDLC was investigated using cyclic voltammetry (CV) and electrochemical impedance spectroscopy. Activated carbons from both the pistachio and acorn shells synthesized at 700 °C in argon gas for two hours exhibited better surface textures and porosity. These activated carbons also exhibited more capacitor-like behavior and lower real impedances, indicating that they would have superior performance compared to the activated carbons obtained at 900 °C. This study may be used to integrate some of natural resources into high-tech energy storage applications for sustainable developments.

**Keywords** Natural resources · Activated carbon · EDLC supercapacitor · Energy storage

## 1 Introduction

### 1.1 General background

Electric energy storage devices require some specific feature, such as manufacturability, life span, costs, performance in terms of energy and power density, charging and discharging capacity and rates, and low maintenance and replacement. When compared to the conventional batteries (e.g., lithium-ion batteries, alkaline and lead acid), supercapacitors are able to deliver more specific power. They can also provide

very high life cycles (from 1000 to 10,000) with a wide range of operating temperatures compared to the batteries. Since the supercapacitors can quickly charge and discharge, these systems can provide a backup in a few seconds with a high peak power. Since the main component is carbon, they are more environmentally friendlier as there is no use of heavy metal and toxic disposal issues [1–3].

Because of these features, supercapacitors are promising energy storage devices that have many applications, such as backup memories, hybrid electric vehicles, adjustable-speed drive ride-through, micro-grids, mobile devices and military equipment [1, 2]. Supercapacitors can be classified as either electrical double-layer capacitors (EDLCs) or pseudocapacitors [3]. In the EDLCs, capacitance develops as the result of charges collecting at the electrode–electrolyte interface [3]. In the pseudocapacitors, oxidation–reduction reactions between the electrolyte and electrodes can take place, leading to capacitance for an energy storage [3, 4].

✉ R. Asmatulu  
ramazan.asmatulu@wichita.edu

<sup>1</sup> Department of Mechanical Engineering, Wichita State University, 1845 Fairmount St., Wichita, KS 67260, USA

<sup>2</sup> Department of Electromechanical Engineering Technology, California State Polytechnic University, 3801 W. Temple Ave., Pomona, CA 91768, USA

Various carbon materials are commonly used to construct the EDLC [5]. Graphene has been explored as an electrode material. Chen et al. reported that reduced graphite oxide (RGO) has a good capacitance in aqueous and ionic liquid electrolytes and residual oxygen on the RGO that led to pseudocapacitance, as well [5]. The performance of activated carbon xerogel has also been investigated, which was synthesized from a renewable resource and glucose with a milder hydrodynamic carbonization method employed along with a graphene oxide nanosheet to provide structural support to the gel [6]. Asymmetric supercapacitors can have an extended potential limit for a long operation. Fan et al. reported that the energy and power density of an asymmetric supercapacitor consisting of a graphene/manganese oxide positive electrode and activated carbon nanofiber negative electrode exceeded the requirements of the most other manganese oxide-based supercapacitors [7].

Activated carbon has received considerable attention as an attractive electrode material for supercapacitors because it is a good conductor of electricity with lower resistances and cost-effective, and has a high porosity, leading to a large surface area for a better supercapacitor performance. The carbon precursors from which the activated carbon is derived are mostly petroleum-based products [8]. With the decrease in fossil fuel reserves and production costs, the search for alternative carbon precursors is imminent. Carbon precursors from biomass such as prawn shells, corn and rice husks, egg white protein and waste tea have been explored in the past for synthesizing porous activated carbon [4, 8, 9]. Various biomass sources, such as recycled papers, cotton fabrics, organic wastes and seeds, can be an economically sustainable solution for the synthesis of activated carbon for future energy use.

Gao et al. demonstrated that nitrogen-doped microporous carbon with a good performance as an electrode material for supercapacitors could be obtained from prawn shells. It was reported that activated carbon from waste tea could be used to synthesize a carbon/polyaniline composite electrode, and it was observed that equal quantities of carbon and polyaniline in the composite maximized its performance as an electrode material for a supercapacitor with an aqueous electrolyte [4]. Liu et al. synthesized activated carbon by carbonizing rice husks at 500 °C and activating them with potassium hydroxide (KOH); the electrode showed a high specific capacitance, such as 330 F/g in a 6 mol/L KOH solution [10]. The porosity and hence the surface area depend on the carbonization temperature of the rice husks [11, 12]. Teo et al. demonstrated that high surface area and specific capacitance in a 6 mol/L KOH solution were observed when the carbonization temperature was 850 °C [11]. Van and Thi also showed that carbon from rice husks carbonized at 800 °C and activated with sodium hydroxide yielded greater performance

as an electrode for a supercapacitor in potassium sulfate electrolyte compared to activated carbon obtained at other carbonization temperatures [12]. Waste tires, which pose a real disposal challenge since they are non-biodegradable waste materials, can be recycled to produce activated carbons by pyrolysis in oxygen-free atmosphere and activation processes using  $H_3PO_4$  solution [13]. It was found that activated carbon from waste tires can be a suitable material for supercapacitor electrodes [13].

The type of electrolyte used in the capacitor can also impact its performance. Three types of electrolytes have been explored for supercapacitor applications: aqueous, organic and ionic liquids [14]. It was observed that the highest specific energy was achieved with a carbon electrode when an ionic liquid was used as the electrolyte, compared to aqueous and organic electrolytes [14]. It was demonstrated that laser treatment of the carbon electrode increased the macropores, thereby improving the surface contact between the electrode and the electrolyte, and the addition of redox electrolyte to the system further enhanced the capacitance [15]. Microporous activated carbon in the presence of *N*-butyl-*N*-methylpyrrolidinium bis(trifluoromethanesulfonyl)imide ionic liquid electrolyte demonstrated much better capacitance and cycling capability [2].

## 1.2 Principles of supercapacitor

Most of the supercapacitors work based on the same principles with the conventional electrostatic capacitors or EDLCs [16]. The conventional capacitors are made of two primary conductors, which are divided by a separator of a non-conductive material, called dielectric membrane. Once the electrical potential is applied to the porous surface of the conductors, they are able to store electrical potential energy in the form of electrical charges, which will be later used as a source of energy when needed. In most of the supercapacitors, the surface area of the conductors is considerably higher than conventional capacitors, and charging and discharging capabilities are higher and also tuned [16–18].

Various capacitor models including Helmholtz model, Gouy–Chapman model, Stern model and current model (double layer) have been developed for different capacitors. These models are explained based on the electrical properties that occur at the boundary layer of the solid conductor and electrolyte [16, 17]. Supercapacitors and conventional electrostatic capacitors both have similar structures. Capability of a device for a charge storing per unit voltage is known as capacitance, which is the primary component for the supercapacitor. When the applied voltage ( $V$ ) across the surface of the capacitor is known and the charge ( $\pm Q$ ) stored in a conductor can be calculated, capacitance value can be determined using the equation below:

$$C = \frac{Q}{V} = \epsilon \frac{A}{d}, \quad (1)$$

where  $A$  is the cross-sectional surface area of the conductor,  $d$  is the distance between the conductors and  $\epsilon$  is the dielectric constant of the dielectric material [16]. Also, stored energy ( $E$ ) in a capacitor can be associated with the following equation:

$$E = \frac{1}{2} CV^2. \quad (2)$$

The cyclic voltammetry (CV) technique can be associated with the scan rate (e.g.,  $dE/dt = 100$  mV/s) within potential range (e.g.,  $\pm 0.75$  V). Sometimes, the ohmic resistance drop can be insignificant before the charge transfer resistance, so in this case, the ohmic resistance can be neglected in the measurements and calculations. If the material transport does not affect the redox kinetics of the electrochemical process, the resistance during the transfer can be equal to the pseudocapacitance resistance. Based on the assumptions, the model system can be created using the real capacitance with the resistance in a parallel surface. The equation below can be used to determine the corresponding upper and lower parts of the curve around the potential. This is equal to the open-circuit voltage. Based on the governing equation, anodic current ( $I_a$ ) and cathodic current ( $I_c$ ) can be extrapolated and capacitance ( $C_{dl}$ ) value for a double-layer capacitor can be calculated [16]:

$$\frac{I_a - I_c}{2} = C_{dl} \frac{dE}{dt}. \quad (3)$$

In the present study, the performance of the activated carbon electrodes from pistachio and acorn shells was investigated in the presence of electrolyte solution containing tetraethylammonium tetrafluoroborate (TEABF<sub>4</sub>) and propylene carbonate (PC). The impact of the carbonization temperatures on the porosity of the electrode and capacitance value of the EDLC was also studied in detail. The novelty of this study includes that for the first time, two natural resources which are abundant in most of the locations on the Earth were stabilized, carbonized and activated, and then, the performances of the prepared supercapacitors were determined at the same testing conditions. The fundamental experiences and knowledge gained through the study would be utilized to advance new technologies on developing future energy storage devices and systems.

## 2 Experiment

### 2.1 Materials

*N, N* Dimethylacetamide (DMAC) (reagent grade), potassium hydroxide (KOH), acetone (HPLC grade) and

hydrochloric acid (HCl) (normality 12.1) were purchased from Fisher Scientific, while Tetraethylammonium tetrafluoroborate (Mw 217.06 g/mol), polyvinylidene fluoride (PVDF) (average Mw ~ 180,000) and propylene carbonate (anhydrous 99.7%) were obtained from Sigma-Aldrich. The manufacturer of the lens tissue used for absorbing the electrolyte was ShieldMe®. The separator used in this study was a special thin porous paper manufactured by Sepp Leaf products, Inc. Pistachios were purchased from a local store, and acorn shells were collected from the Wichita State University campus during the fall season. The polyethylene terephthalate (PET) was manufactured by M. G. Chemicals Ltd. All the materials and chemicals were used in the present study without further modifications, unless otherwise specified.

## 2.2 Methods

### 2.2.1 Carbonization and chemical activation

The activated carbons were produced from pistachio and acorn shells, which were washed several times and soaked in deionized (DI) water overnight. Then, they were dried in an oven (Precision Scientific/Thelco Laboratory Oven) for two hours at 105 °C to remove any excess water and further heated to 240 °C at 5 °C/min (stabilization step) for two hours to remove any volatile content from the shells in an ambient condition. The shells were then soaked in 1 wt% KOH solution and stored in a vacuum desiccator for 30 min at 22 in. Hg pressure to remove trapped air, followed by soaking in the KOH solution again for another 12 h for chemical activation process. The shells were then collected and dried in an oven at 85 °C for two hours. A portion of the shells was carbonized in a tube furnace (MTI Corporation/OTF – 1200X) at 700 °C, and the remaining portion was carbonized at 900 °C for two hours at 5 °C/min heating rate under an argon gas flow. Based on our previous studies on carbonization studies, these are the optimum temperature for the selected biomasses. For example, 500 °C was not sufficient to make highly porous and carbonized structures while over 1000 °C process temperature makes the structures unsuitable for the capacitor applications. An inert environment was necessary to prevent oxidation at higher temperatures. The carbonized shells were washed three times with a 36% HCl solution to neutralize any remaining KOH in the pores, followed by washing with DI water to remove the acid content. The carbonized shells were heated again to 105 °C for two hours to remove any water remaining in the pores. The activated carbons were collected and ground for 30 min using a mortar and pestle to make carbon electrodes. The activated carbon from pistachio shells was designated as either P700AC or P900AC, where P refers to pistachio and the number following it indicates the activation temperature.

Similarly, the activated carbon from acorn shells was designated as K700AC and K900AC, where K refers to acorn shells [16, 17]. Figure 1 shows the images of the pistachio and acorn shells, and pistachio shells after carbonization and activation.

### 2.2.2 Construction of electrodes and electrolytes

Using a tape, a layout of  $2 \times 2 \times 0.13$  cm in size was created on an aluminum foil (conductive layer). PVDF (5 wt%) was mixed with DMAC and acetone (70:30 weight ratio) using a magnetic stirrer for 4 h at 50 °C. The activated carbon powders were added into the PVDF solution (50:50 weight ratio) and stirred for 5 min using a magnetic stirrer. The resulting thick slurry was then applied to the layout on the aluminum foil to construct a thin layer of activated carbon electrodes. The electrodes were then heated in an oven at 120 °C for four hours to dry the mixture/paste, which was turned into a solid/robust electrode.

The high temperature made the electrode structure more robust. The electrolyte consisted of 1 M TEABF<sub>4</sub> with PC as the solvent. The lens tissue was soaked into this electrolyte mixture and stored in the vacuum desiccator for 30 min.

### 2.2.3 Construction of supercapacitor

The supercapacitor was constructed by assembling the electrode and the electrolyte. The activated carbon was placed on a PET sheet, and the soaked lens tissue was placed on top of the electrode. The separator, or thin porous paper, was placed on top of the soaked lens tissue. Another similar symmetric assembly was constructed, and the two parts were put together to form the supercapacitor. Figure 2 shows the assembly layers and the complete supercapacitor for the performance testing.



**Fig. 1** Images showing **a** the pistachio shells, **b** acorn shells, **c** pistachio shells after carbonization and **d** the same pistachio shells after activation with KOH solutions prior to the grinding

### 2.2.4 SEM analysis

The surface morphology of the activated carbon powders from pistachio and acorn shells was characterized using Zeiss Sigma variable pressure field emission scanning electron microscopy (SEM). The specimen was sputter-coated with gold to make it more conductive for a better imaging. Gold coating was not used in another assembly process of supercapacitors.

### 2.2.5 Cyclic voltammetry study

In a cyclic voltammetry study, the applied potential was increased from one specific point to the other one at a constant rate and then decreased back to its initial potential at the same scan rate. The CV was employed to study the electron transfer kinetics, transport properties, oxidation peaks, etc. The performance of the supercapacitors was studied using cyclic voltammetry of the BioLogic SP-150 potentiostat/galvanostat at various scan rates (10 mV/s, 20 mV/s, 50 mV/s, 100 mV/s, 150 mV/s, 200 mV/s, 250 mV/s, 300 mV/s, 400 mV/s and 500 mV/s). During the cyclic voltammetry study, a constant pressure of 82.41 g/cm<sup>2</sup> was applied to ensure proper contact between various components of the EDLC. A voltammogram plot was constructed from the data collected for each electrode type: P700, P900, K700 and K900.

### 2.2.6 EIS analysis of supercapacitors

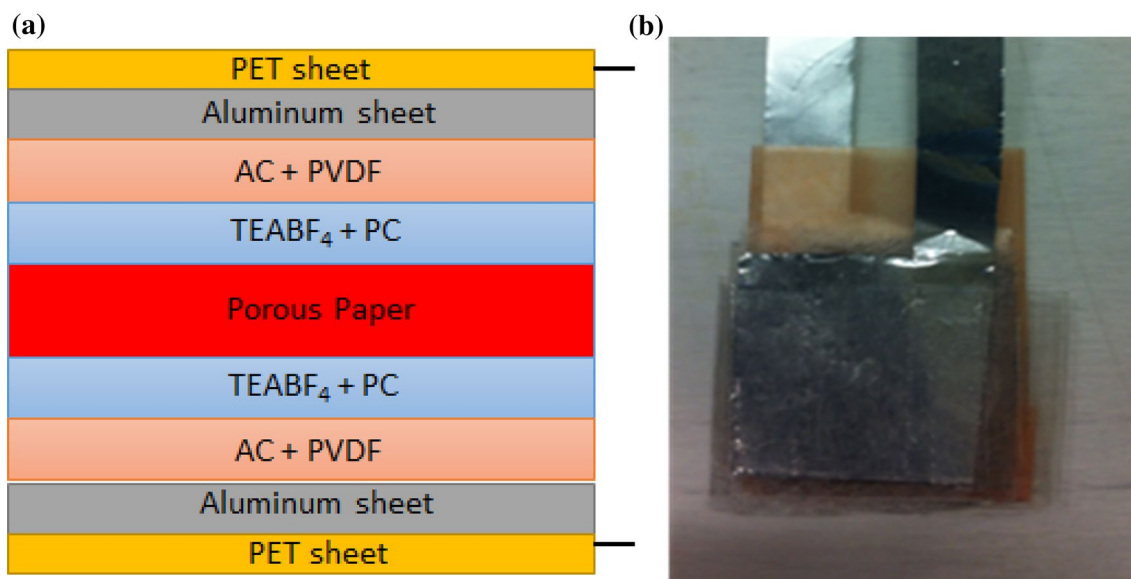
Electrochemical impedance spectroscopy (EIS) is a common technique to study the motion of ions in devices such as

batteries and supercapacitors and catalytic reaction kinetics. Here, the impedance of a device is determined as a function of frequency rates. A small sinusoidal potential at various frequencies was applied along with a constant direct potential signal, and the impedance change was continuously recorded. The EIS was carried out using a Gamry Series G300TM potentiostat/galvanostat/ZRA. For this study, the frequency was varied from 10 Hz to 300 kHz. The root mean square potential of the alternating signal was 1000 mV, and the direct potential was 1 V. During the EIS tests, a constant pressure of 82.41 g/cm<sup>2</sup> was also applied on the device to ensure that all components were in good contact with each other. Each experiment was repeated at least five times, and the test results were averaged.

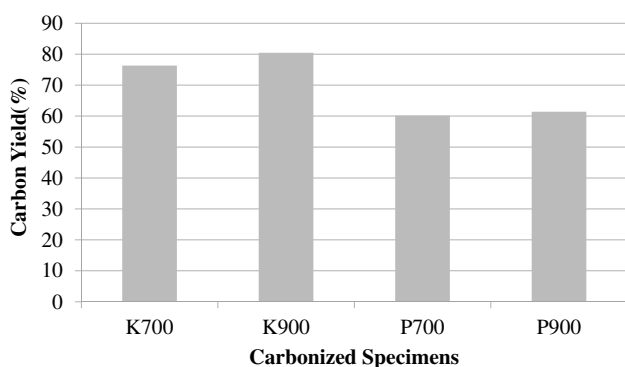
## 3 Results and discussion

### 3.1 Carbon yields and SEM analysis

In order to analyze the carbon yields of the pistachio and acorn shells, both samples were weighted before and after the carbonization processes. Figure 3 shows the carbon yields of pistachio and acorn shells after the carbonizations at 700 and 900 °C for 2 h in argon gas. The test results also showed that acorn shells provided about 16–20% higher percentage of carbon yield than pistachio shells. There is a slight difference between 700 and 900 °C on the carbon yield. The carbon yields before and after the KOH treatments were similar to each other. This process may be more economical to produce larger quantities of activated carbons from the acorn shells.



**Fig. 2** Construction of EDLC: **a** schematic views of various components and **b** assembled supercapacitor with activated carbon electrodes



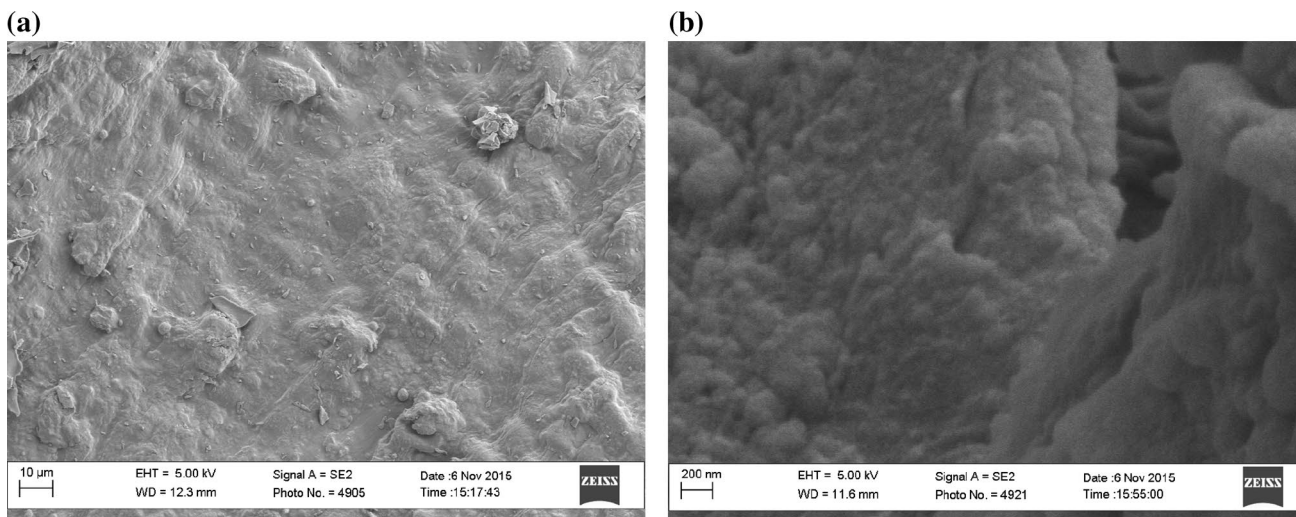
**Fig. 3** Carbon yields of pistachio and acorn shells after the carbonizations at 700 and 900 °C for 2 h

Figure 4 shows the SEM images of carbonized acorn and pistachio shells produced at 700 °C for 2 h in argon gas flow before the activation process. As can be seen on the SEM images, carbonized samples did not provide too much surface structural changes and look alike more solid with very less pore formations. This will greatly reduce the overall surface area and charge storing capacity of the supercapacitors and their energy storage capabilities. In order to increase the surface area of the carbon electrodes, the activation is a necessary process for the supercapacitor building.

Figure 5 illustrates the SEM images of the activated acorn shells K700AC at 700 °C with 200 nm magnification, cross section of the same activated shells at 1 μm and 10 μm magnifications and ground carbon electrode powders made from the K700AC shells. The effects of activation process can be analyzed using the SEM images of the

carbonized shells. Huge surface area was created after the activation process. The porous structures can be noticed all over the surfaces, which could be beneficial for the energy storing capacity of the supercapacitors. Figure 6 also reveals the SEM images of activated acorn K900AC shells at 900 °C with the same magnifications and ground carbon electrode made from the K900AC shells. Comparing the images, it can be seen that the pores for K900AC activated carbon are larger than those for K700AC, indicating that the process parameters can drastically affect the surface texture and morphology. The similar surface texture/structures were seen on the other shells.

Figure 7 exhibits the SEM images of activated pistachio P900AC shells produced at 900 °C with high (1 μm) and low (10 μm) magnifications. Both SEM images indicated that the activated pistachio shells have substantial structural changes after the KOH activation process, and porosity and surface textures were completely changed. Similar observations were also seen on the pistachio samples carbonized at 700 °C for 2 h in the inert gas. Generally, the SEM images confirmed that the activation of carbons by the KOH solution enhanced the surface area, porosity and texture for both carbonized acorn and pistachio. This may be the primary reason of having higher supercapacitor storage capacity. During the carbonization and activation processes, liquid and gas in the structures of the pistachio and acorn were released and amorphous parts of the carbon tend to be recrystallized (or semi-recrystallized). X-ray diffraction (XRD) and Brunauer–Emmett–Teller (BET) surface area studies will be conducted in our future studies to analyze the crystalline structures of the carbonized and activated shells and real surface area values.



**Fig. 4** SEM images of carbonized **a** acorn (K700) and **b** pistachio (P700) shells before the activation process

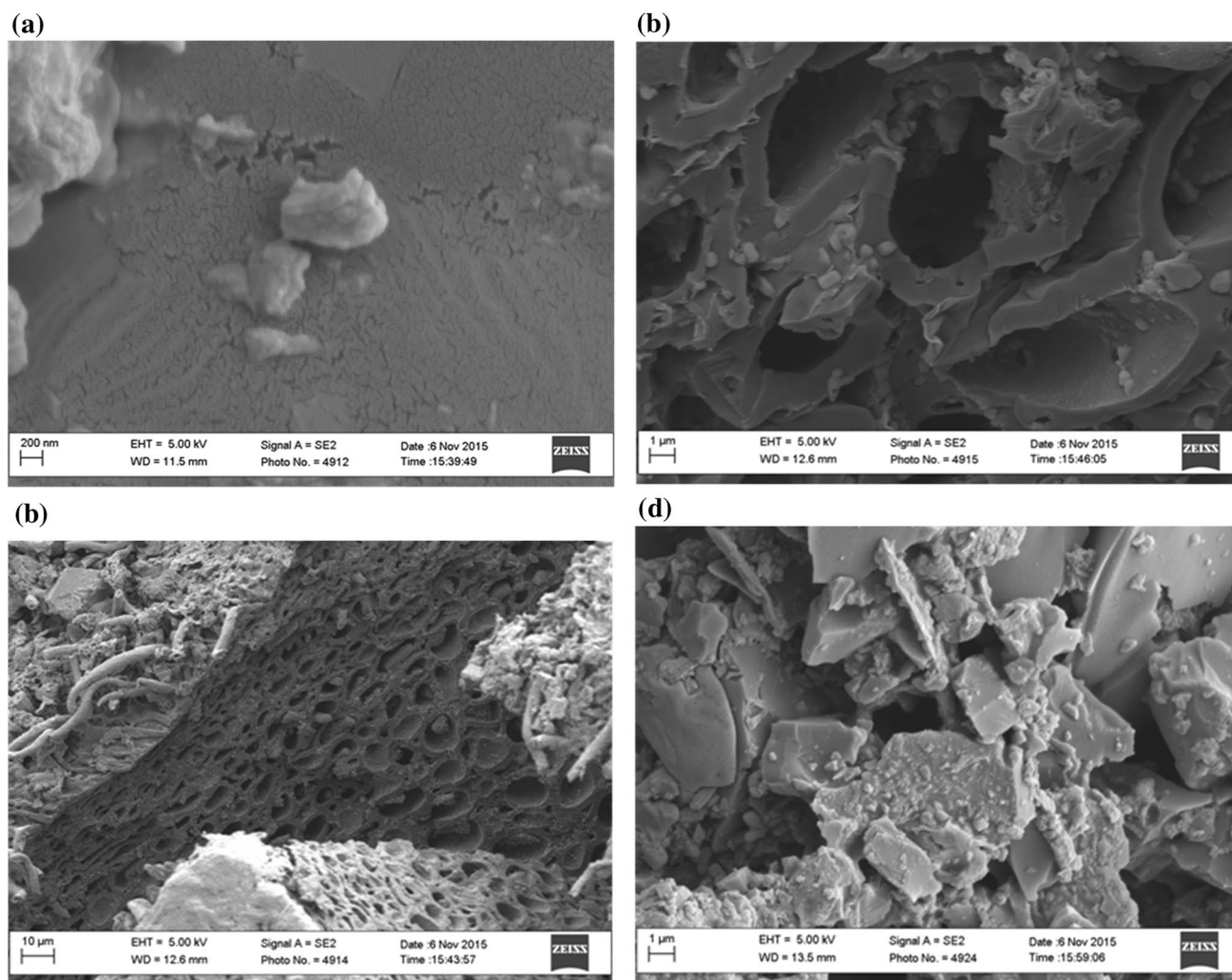


**Fig. 5** SEM images of activated acorn K700AC shells at **a** 200 nm magnification, cross section of the same activated shells at **b** 1  $\mu\text{m}$  and **c** 10  $\mu\text{m}$  magnifications and **d** ground carbon electrode made from the activated K700AC shells

### 3.2 Cyclic voltammetry studies

Cyclic voltammetry is a scientific approach for the electrochemical analysis of capacitors, supercapacitors and batteries which involves in scanning of the potential of a stationary working electrode using a triangular potential waveform. Through the potential sweep, the potentiostat measures the currents of the supercapacitors and defines the voltage vs current behaviors. Following the theory, one can determine the capacitance values of the supercapacitors. In an ideal capacitor, the outcome of the cyclic voltammogram can be in rectangular shape, but in reality there are some resistances in the real capacitor, which can provide parallelogram or similar shapes depending on the structural elements used in the supercapacitors and properties of the electrode materials [16–19]. Supercapacitors made with different activated carbon structures

were analyzed using cyclic voltammetry to determine their performances.

Figures 8 and 9 show the cyclic voltammograms for K700AC, K900AC, P700AC and P900AC at the selected scan rates of 10 mV/s, 100 mV/s and 500 mV/s, respectively. In the graphs, *X*-axis represents potential and *Y*-axis represents current values. As expected, the total current increased with the increasing scan rates. With the increasing scan rate, the diffusion layer grew closer to the electrodes, which meant that the flux density at the electrode surface also increases. This led to an increased current with the scan rate on the activated electrode surfaces. The voltammograms for P700AC and K700AC electrodes exhibit a box-like shape, indicating a good capacitor-like behavior. The shape of the cyclic voltammogram becomes more distorted for the P900AC and K900AC samples, thus indicating instability at the electrode/electrolyte interface. Among all the cyclic

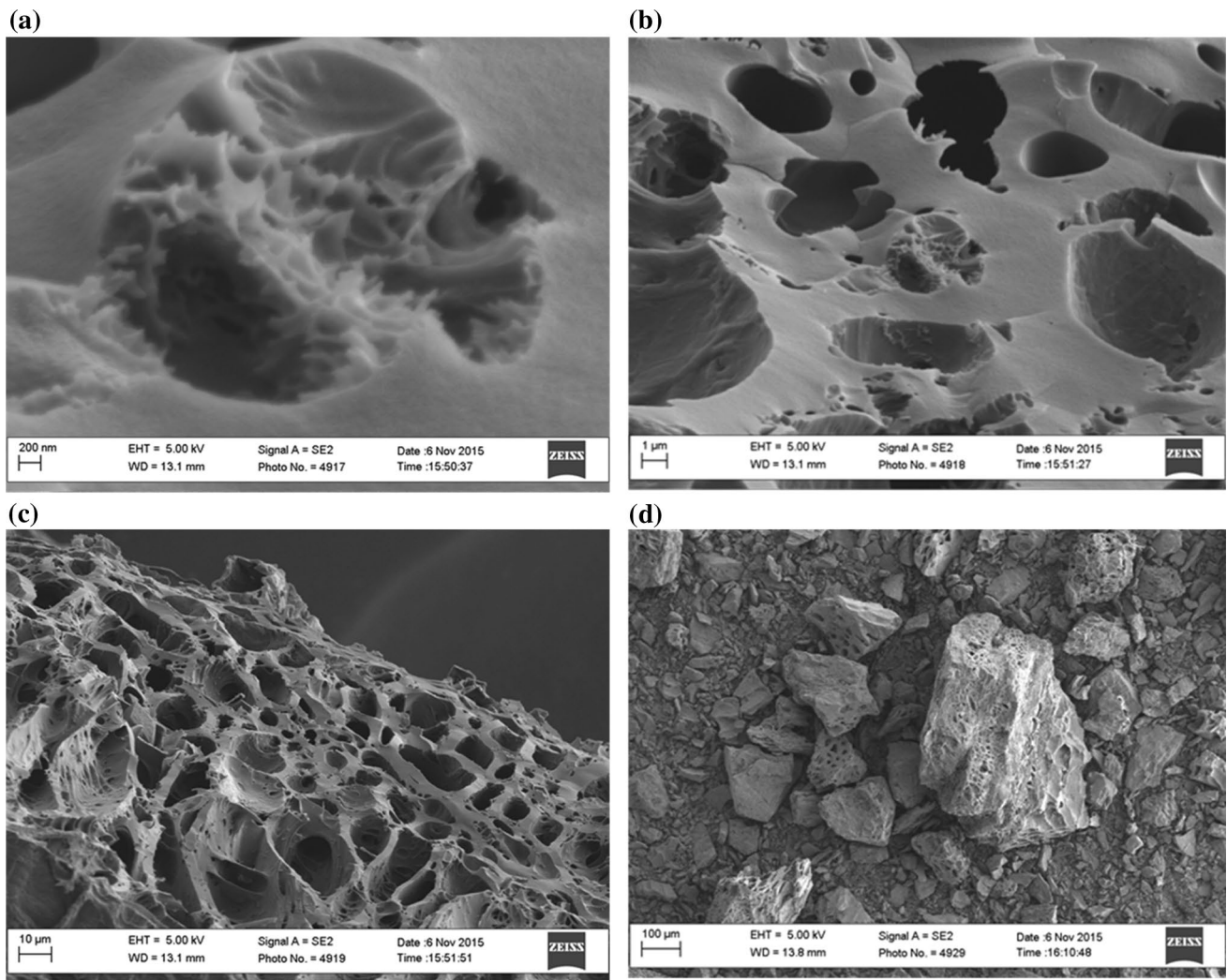


**Fig. 6** SEM images of activated acorn K900AC shells at 900 °C with **a** 200 nm magnification, cross section of the same activated shells of **b** 1 μm and **c** 10 μm magnifications and **d** ground carbon electrode made from the activated K900AC shells

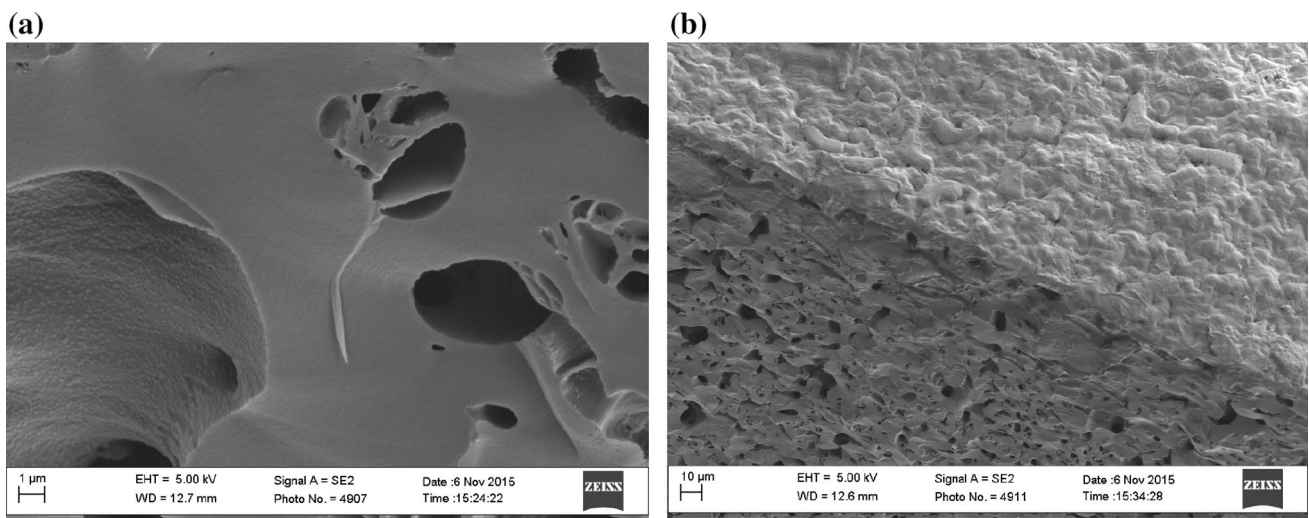
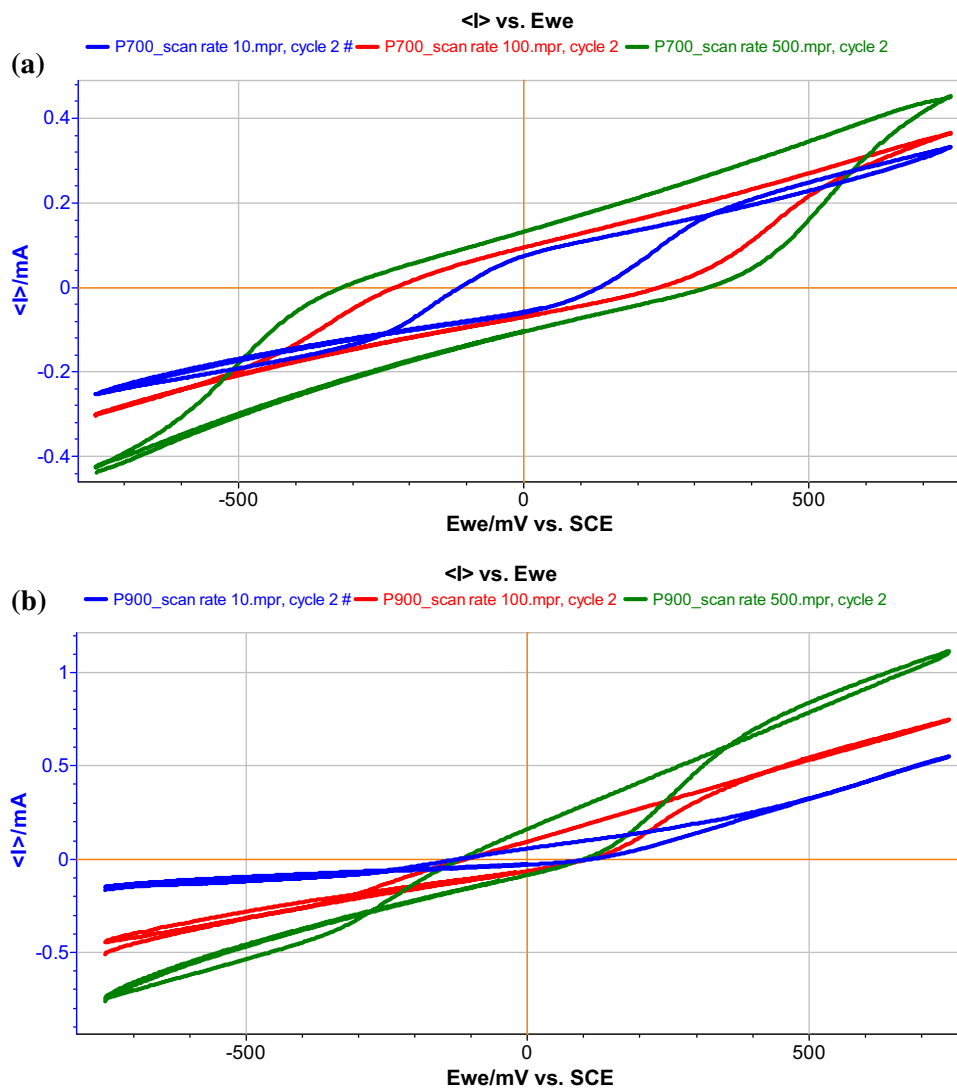


**Fig. 7** SEM images of activated pistachio P900AC shells produced at 900 °C with **a** 1 μm and **b** 10 μm magnifications



**Fig. 8** Cyclic voltammograms of **a** P700AC and **b** P900AC at scan rates of 10 mV/s, 100 mV/s and 500 mV/s



voltammogram studies, the sample K700AC seems to give the better performance for supercapacitor applications. At higher temperatures, some physical and chemical changes (e.g., porosity, local melting, crystallinity, density, etc.) and chemical reactions likely took place to change the cyclic voltammogram behavior of the substrates.

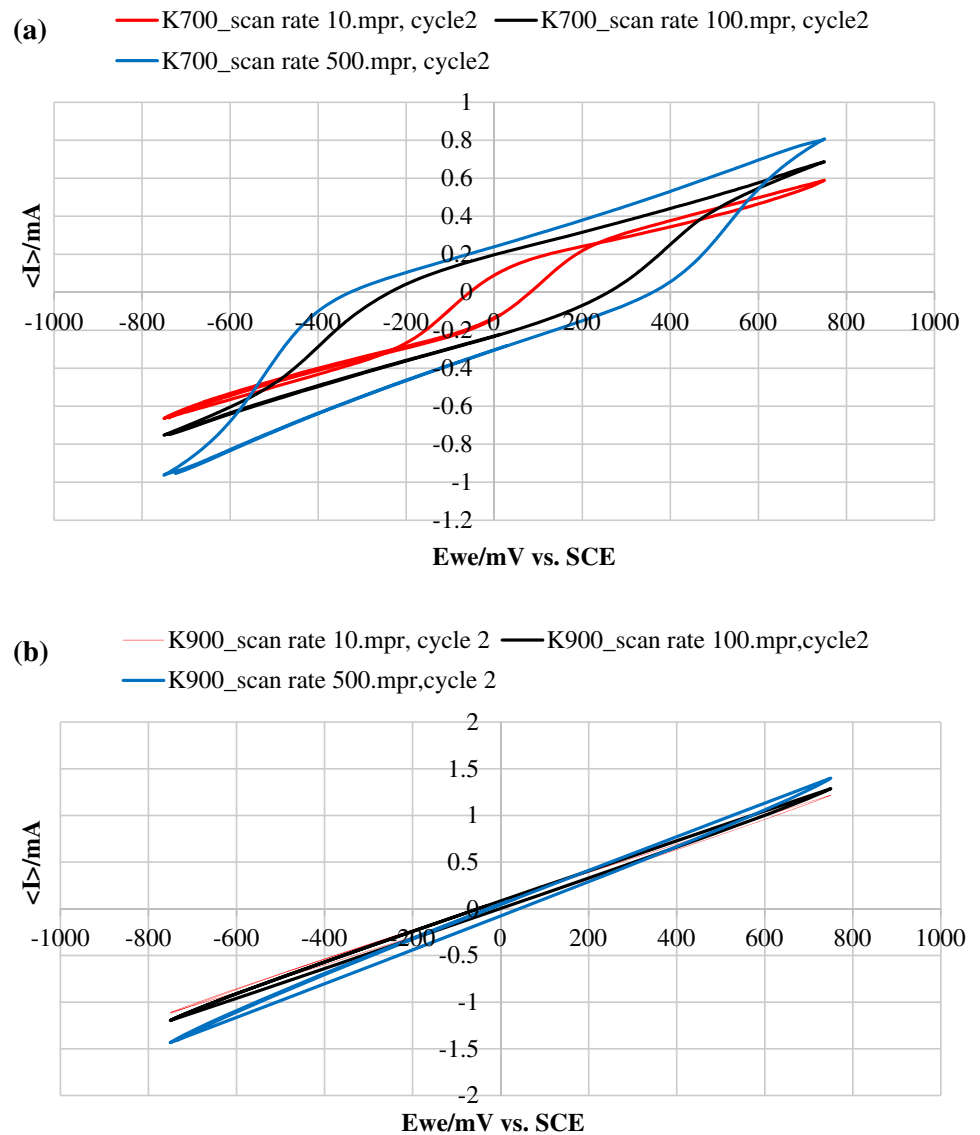
### 3.3 Specific capacitance of supercapacitors

The steady-state curves of current ( $I$ ) vs. potential ( $E_{we}$ ) for forward and backward voltage scans of the activated carbon materials were determined, and then, specific values of the prepared supercapacitors were calculated as shown in Eq. 3. Figure 10 shows the curves of  $I$  vs.  $E_{we}$  for forward and backward voltage scan of the activated acorn K700AC. Using the equation and graphics, anodic and cathodic currents can be extrapolated and the specific capacitance for the supercapacitor can be calculated [16]. From Fig. 10,

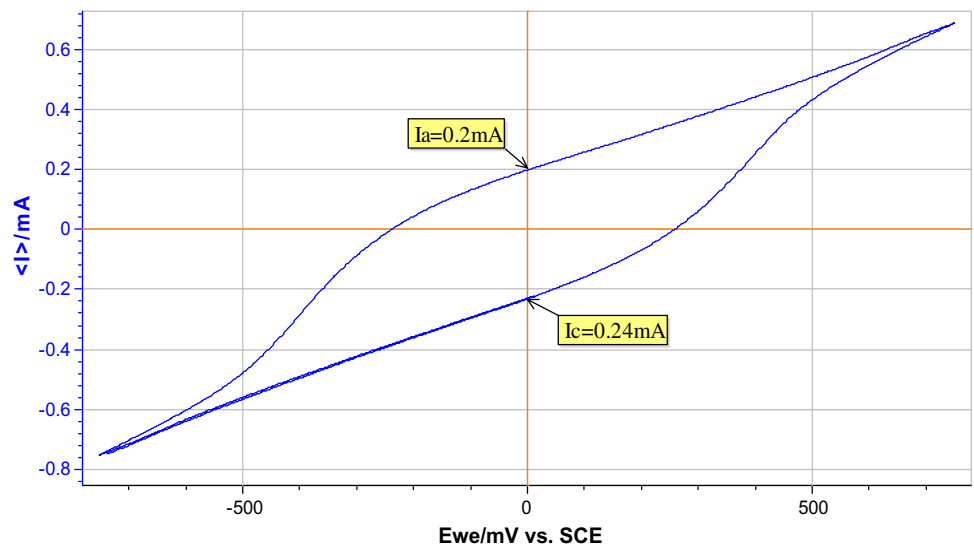
anodic (0.2 mA) and cathodic (0.24 mA) currents can be determined, and specific capacitance ( $C_s$ ) value (9166.67  $\mu\text{F/g}$ ) can be calculated with the capacitance (2200  $\mu\text{F}$ ) value divided by sample weight (0.24 g). All the specific capacitance calculations were followed through the same procedure.

Figure 11 displays the specific capacitance values of four supercapacitors made of the activated P700AC, P900AC, K700AC and K900AC samples as a function of different scan rates. The test results indicated that the specific capacitance values of the samples were decreased when the scan rates in the cyclic voltammetry curves were increased. After analyzing the test results, it was found out that the P700AC and K700AC samples showed higher specific capacitance values when compared to the P900AC and K900AC samples. Among all the activated samples, K700AC sample provided the highest specific capacitance values for all the scan rates, which was expected after observing

**Fig. 9** Cyclic voltammograms of **a** K700AC and **b** K900AC supercapacitors at scan rates of 10 mV/s, 100 mV/s and 500 mV/s



**Fig. 10** Steady-state curve  $I$  vs.  $E_{we}$  for forward and backward voltage scan of the activated acorn K700AC sample



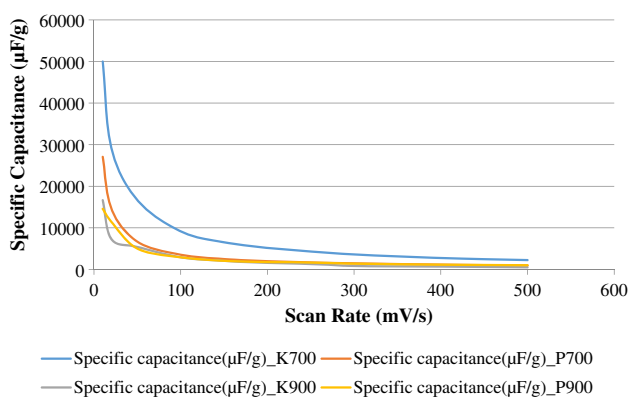


**Fig. 11** Specific capacitance values of four supercapacitors built using the activated P700AC, P900AC, K700AC and K900AC samples as a function of different scan rates

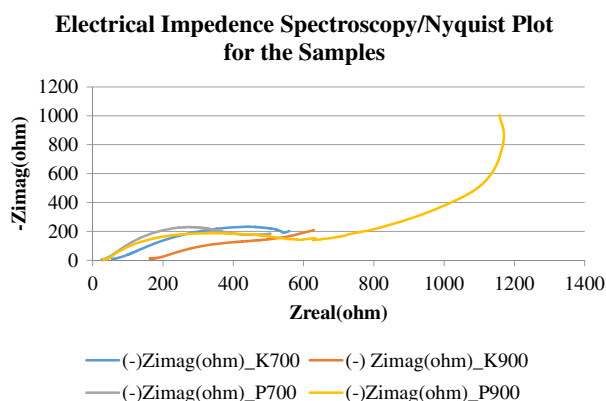


**Fig. 12** EIS values of the activated K700A, K900AC, P700AC and P900AC samples

the cyclic voltammogram test results. At the lowest scan rate of 10 mV/s, K700AC and P700AC samples showed 50,000  $\mu\text{F/g}$  and 27,083  $\mu\text{F/g}$ , while K900AC and P900AC samples showed 17,450  $\mu\text{F/g}$  and 14,300  $\mu\text{F/g}$  of specific capacitances, correspondingly.

### 3.4 EIS analysis

Figure 12 shows the EIS (or Nyquist plot) values of the activated K700AC, K900AC, P700AC and P900AC electrodes. The real impedance values of the P700AC, P900AC, K700AC and K900AC electrodes were approximately 440, 600, 540 and 520  $\Omega$ , respectively. It is seen that the P700AC sample provided the lowest real impedance value of 440  $\Omega$ , whereas the P900AC samples gave the highest real impedance value of 600  $\Omega$ . According to this study, the P700AC electrode has the smallest electrical energy loss with a very high specific capacitance. The second lowest electrical energy loss was from the K700AC electrode. The acorn and

pistachio shells carbonized at 900  $^{\circ}\text{C}$  exhibited the higher real impedance values and hence incurred the higher energy losses during the energy storage. Furthermore, other than the electrode K900AC, the activated carbon electrodes of P700AC and K700AC provided better semicircular behavior at high frequency ranges, implying that these samples should provide good capacitive behavior at high frequency values. Also, the sample P900AC can provide somewhat better results than K900AC sample. Based on the Nyquist plots, it is concluded that the acorn and pistachio shells carbonized at 700  $^{\circ}\text{C}$  for 2 h in argon gas followed by the KOH activation process can be used to fabricate new class of natural resource-based supercapacitors [16]. From this study, it is also determined that the cyclic voltammetry, specific capacitance and EIS studies are mainly in good agreement with each other.

Overall, this study shows that activated carbons from pistachio and acorn shells can be an alternative precursor for activated carbon electrode materials. It was observed that both K700AC and P700AC exhibited a more capacitor-like behavior and lower real impedances, indicating that they would have superior performance compared to the activated carbon obtained at 900  $^{\circ}\text{C}$ . The greater performances of the P700AC and K700AC electrodes can be attributed to the higher porosity and surface area within the carbon structures when compared to the other electrodes. The lower performances of the other two electrodes can be attributed to the disordered and damaged structures at such a high temperature, thus causing the porosity and other structural changes [19–23]. High porosity within the electrode material allows more charge movement and enhanced contact between the electrolyte and electrode. Hence, carbonization at the higher temperatures can negatively impact the performance of the electrode materials.

## 4 Conclusions

In this study, the performances of activated carbons from the natural resources such as acorn and pistachio shells as electrode materials were investigated for supercapacitor applications. It was observed that there is a limit for the carbonization temperature in order to obtain a desirable performance of the activated carbons. Here, better performance of the electrode was observed when the carbonization temperature was 700  $^{\circ}\text{C}$  when compared to 900  $^{\circ}\text{C}$ . The carbonization temperature can impact the porosity and performance of the supercapacitors drastically. Activation by KOH solution is a necessary process to improve the capacitance values of the supercapacitors. The cyclic voltammograms, specific capacitance and EIS studies also confirmed that low temperature (700  $^{\circ}\text{C}$ ) carbonization followed by KOH activation had the major contribution on the supercapacitor performances.

Overall, this study confirms that natural resources have a great potential to be used as a precursor material for building new generations of EDLC-based supercapacitors after appropriate physical and thermal treatment processes.

**Acknowledgements** The authors gratefully acknowledge the Kansas NSF EPSCoR (#R51243/700333) and Wichita State University for the financial and technical support of this work.

## References

- Bingbing W, Zhongdong Y, Xiangning X (2010) Super-capacitors energy storage system applied in the microgrid. In: Industrial electronics and applications (ICIEA), 2010 the 5th IEEE Conference on. IEEE, pp 1002–1005
- Balducci A, Dugas R, Taberna P-L et al (2007) High temperature carbon-carbon supercapacitor using ionic liquid as electrolyte. *J Power Sources* 165:922–927
- Du X, Wang C, Chen M, Jiao Y, Wang J (2009) Electrochemical performances of nanoparticle Fe<sub>3</sub>O<sub>4</sub>/activated carbon supercapacitor using KOH electrolyte solution. *J Phys Chem C* 113:2643–2646
- Inal IIG, Gokce Y, Aktas Z (2016) Waste tea derived activated carbon/polyaniline composites as supercapacitor electrodes. In: Renewable energy research and applications (ICRERA), 2016 IEEE International Conference on. IEEE, pp 458–462
- Chen Y, Zhang X, Zhang D, Yu P, Ma Y (2011) High performance supercapacitors based on reduced graphene oxide in aqueous and ionic liquid electrolytes. *Carbon* 49:573–580
- Chen Y, Zhang X, Zhang D, Ma Y (2012) High power density of graphene-based supercapacitors in ionic liquid electrolytes. *Mater Lett* 68:475–477
- Fan Z, Yan J, Wei T et al (2011) Asymmetric supercapacitors based on graphene/MnO<sub>2</sub> and activated carbon nanofiber electrodes with high power and energy density. *Adv Funct Mater* 21:2366–2375
- Gao F, Qu J, Zhao Z, Wang Z, Qiu J (2016) Nitrogen-doped activated carbon derived from prawn shells for high-performance supercapacitors. *Electrochim Acta* 190:1134–1141
- Li Z, Xu Z, Tan X et al (2013) Mesoporous nitrogen-rich carbons derived from protein for ultra-high capacity battery anodes and supercapacitors. *Energy Environ Sci* 6:871–878
- Liu D, Zhang W, Lin H, Li Y, Lu H, Wang Y (2016) A green technology for the preparation of high capacitance rice husk-based activated carbon. *J Clean Prod* 112:1190–1198
- Teo EYL, Muniandy L, Ng E-P et al (2016) High surface area activated carbon from rice husk as a high performance supercapacitor electrode. *Electrochim Acta* 192:110–119
- Le Van K, Thi TTL (2014) Activated carbon derived from rice husk by NaOH activation and its application in supercapacitor. *Prog Nat Sci Mater Int* 24:191–198
- Zhi M, Yang F, Meng F, Li M, Manivannan A, Wu N (2014) Effects of pore structure on performance of an activated-carbon supercapacitor electrode recycled from scrap waste tires. *ACS Sustain Chem Eng* 2:1592–1598
- Lewandowski A, Olejniczak A, Galinski M, Stepniak I (2010) Performance of carbon-carbon supercapacitors based on organic, aqueous and ionic liquid electrolytes. *J Power Sources* 195:5814–5819
- Hwang JY, Li M, ElKady MF, Kaner RB (2017) Next-generation activated carbon supercapacitors: a simple step in electrode processing leads to remarkable gains in energy density. *Adv Funct Mater* 27:1605745
- Faisal MSS (2015) Studying activated carbons of natural sources for supercapacitor applications. MS Thesis, Wichita State University
- Faisal MSS, Rahman MM, Asmatulu R (2016) Investigating effectiveness of activated carbons of natural sources on various supercapacitors. In: Smart materials and nondestructive evaluation for energy systems 2016. International Society for Optics and Photonics, p 9
- Choi JE, Ko S, Jeon YP (2019) Preparation of petroleum impregnating pitches from pyrolysis fuel oil using two-step heat treatments. *Carbon Lett* 29:369–376
- (2015) Basics of electrochemical impedance spectroscopy Gamry instruments. Retrieved 2015. <https://www.gamry.com/application-notes/EIS/>
- Jabbarnia A, Khan W, Ghazinezami A, Asmatulu R (2016) Tuning the ionic and dielectric properties of electrospun nanocomposite fibers for supercapacitor applications. *Int J Eng Res Appl* 6:65–73
- Jabbarnia A, Khan WS, Ghazinezami A, Asmatulu R (2016) Investigating the thermal, mechanical, and electrochemical properties of PVdF/PVP nanofibrous membranes for supercapacitor applications. *J Appl Polym Sci* 133
- Jabbarnia A, Asmatulu R (2015) Synthesis and characterization of PVdF/PVP-based electrospun membranes as separators for supercapacitor applications. *J Mater Sci Technol Res* 2:43–51
- Baek J, Lee HM, An KH, Kim BJ (2019) Preparation and characterization of highly mesoporous activated short carbon fibers from Kenaf precursors. *Carbon Lett* 29:393–399

**Publisher's Note** Springer Nature remains neutral with regard to jurisdictional claims in published maps and institutional affiliations.